

# Bioinspired Collagen Scaffold Loaded with bFGF-Overexpressing Human Mesenchymal Stromal Cells Accelerating Diabetic Skin Wound Healing via HIF-1 Signal Pathway Regulated Neovascularization

Feifei Huang,<sup>†</sup> Tianyun Gao,<sup>†</sup> Yirui Feng,<sup>†</sup> Yuanyuan Xie, Chenxu Tai, Yahong Huang,\* Li Ling,\* and Bin Wang\*



Cite This: *ACS Appl. Mater. Interfaces* 2024, 16, 45989–46004



Read Online

ACCESS |



Metrics & More



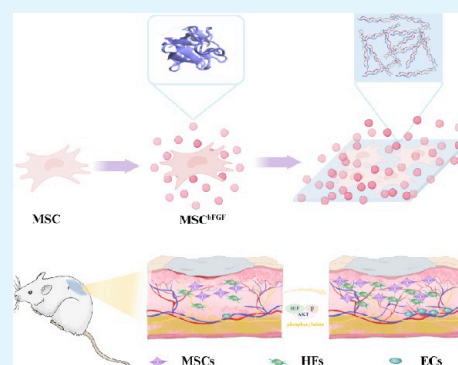
Article Recommendations



Supporting Information

**ABSTRACT:** The healing of severe chronic skin wounds in chronic diabetic patients is still a huge clinical challenge due to complex regeneration processes and control signals. Therefore, a single approach is difficult in obtaining satisfactory therapeutic efficacy for severe diabetic skin wounds. In this study, we adopted a composite strategy for diabetic skin wound healing. First, we fabricated a collagen-based biomimetic skin scaffold. The human basic fibroblast growth factor (bFGF) gene was electrically transduced into human umbilical cord mesenchymal stromal cells (UC-MSCs), and the stable bFGF-overexpressing UC-MSCs (bFGF-MSCs) clones were screened out. Then, an inspired collagen scaffold loaded with bFGF-MSCs was applied to treat full-thickness skin incision wounds in a streptozotocin-induced diabetic rat model. The mechanism of skin damage repair in diabetes mellitus was investigated using RNA-Seq and Western blot assays. The bioinspired collagen scaffold demonstrated good biocompatibility for skin-regeneration-associated cells such as human fibroblast (HFs) and endothelial cells (ECs). The bioinspired collagen scaffold accelerated the diabetic full-thickness incision wound healing including cell proliferation enhancement, collagen deposition, and re-epithelialization, compared with other treatments. We also showed that the inspired skin scaffold could enhance the *in vitro* tube formation of ECs and the early angiogenesis process of the wound tissue *in vivo*. Further findings revealed enhanced angiogenic potential in ECs stimulated by bFGF-MSCs, evidenced by increased AKT phosphorylation and elevated HIF-1 $\alpha$  and HIF-1 $\beta$  levels, indicating the activation of HIF-1 pathways in diabetic wound healing. Based on the superior biocompatibility and bioactivity, the novel bioinspired skin healing materials composed of the collagen scaffold and bFGF-MSCs will be promising for healing diabetic skin wounds and even other refractory tissue regenerations. The bioinspired collagen scaffold loaded with bFGF-MSCs could accelerate diabetic wound healing via neovascularization by activating HIF-1 pathways.

**KEYWORDS:** bFGF, mesenchymal stromal cells, collagen scaffold, diabetic wound healing



The bioinspired collagen scaffold loaded with bFGF-MSCs accelerated the diabetic full-thickness incision wound healing including cell proliferation enhancement, collagen deposition, and re-epithelialization, compared with other treatments. We also showed that the inspired skin scaffold could enhance the *in vitro* tube formation of ECs and the early angiogenesis process of the wound tissue *in vivo*. Further findings revealed enhanced angiogenic potential in ECs stimulated by bFGF-MSCs, evidenced by increased AKT phosphorylation and elevated HIF-1 $\alpha$  and HIF-1 $\beta$  levels, indicating the activation of HIF-1 pathways in diabetic wound healing. Based on the superior biocompatibility and bioactivity, the novel bioinspired skin healing materials composed of the collagen scaffold and bFGF-MSCs will be promising for healing diabetic skin wounds and even other refractory tissue regenerations. The bioinspired collagen scaffold loaded with bFGF-MSCs could accelerate diabetic wound healing via neovascularization by activating HIF-1 pathways.

## INTRODUCTION

Currently, more than 420 million individuals globally are diagnosed with diabetes. Projections indicate that this number will increase to approximately 578 million by 2030 and further rise to 700 million by 2045.<sup>1</sup> Due to the increasing prevalence of diabetes mellitus all around the world, a wide range of complications have occurred during the course of this disease.<sup>2</sup> Among them, about 20% of the patients suffer from the diabetic skin wound,<sup>3,4</sup> which is associated with a series of micro- and macrovascular lesions, leading to limb loss and disability in severe cases. The normal wound healing process could be divided into three stages according to time-dependent stages (inflammation, proliferation, and matrix remodeling stages).<sup>5</sup> Vascular delivery of nutrition and oxygen is the most crucial factor in healing process of all the three stages.<sup>6</sup> Generally, the refractory diabetic wound is mainly due to the abnormal glucose

metabolism which leads to impaired blood microcirculation, anomalous inflammatory response, peripheral neuropathy, abnormal expressions of matrix metalloproteinases, and vascular endothelial growth factors affecting the vascular support for the wound healing.<sup>7</sup>

The traditional clinical managements for diabetes-related trauma are focused on late dressing changes, negative pressure, electrical stimulation, hyperbaric oxygen, and skin grafting.

**Received:** May 19, 2024

**Revised:** August 6, 2024

**Accepted:** August 8, 2024

**Published:** August 21, 2024



However, the treatment outcomes for severe skin lesions remain unsatisfactory. At present, the application of many new technologies and materials brings more possibilities for the complete healing of diabetic skin trauma. Mesenchymal stromal cells (MSCs) are widely applied to treat a variety of complications due to the potentials to differentiate into multiple lineage cells, modulate the immune functions, and secrete relevant growth factors.<sup>8</sup> Human umbilical cord derived MSCs (UC-MSCs) are the most widely used MSCs and have been shown to increase angiogenesis, reduce apoptosis, modulate the immune response and remodel the extracellular matrix micro-environment to accelerate wound closure in diabetic wounds.<sup>9</sup>

Multiple cytokines play an important role in wound healing. Typically, the basic fibroblast growth factor (bFGF) involved in the proliferative phase of wound repair could promote diabetic wound healing via a faster vascularization and better cell proliferation promotion.<sup>10</sup> However, some limitations of cytokines including bFGF such as short half-life *in vivo*, efficient delivery into lesions, and heavy costs hamper the efficacy of refractory skin wound healing.<sup>11,12</sup> Therefore, cytokine engineered MSCs could resolve these disadvantages.<sup>13–15</sup>

Diabetic wound healing is involved in complex processes and control signals. In clinic, a single method is difficult to obtain satisfactory therapeutic efficacy for diabetic skin wounds, and a combination of various approaches are promising to achieve complete healing of diabetic wounds.<sup>16</sup> Collagen, a major component of the extracellular matrix (ECM), is a structural protein with significant tensile strength that facilitates cell adhesion, proliferation, differentiation, and tissue development. In comparison to other material scaffolds, the advantages of collagen scaffolds are low antigenicity, good biocompatibility and biodegradability, superior mechanical stability, and structural support for cell growth. In this study, we first fabricated a collagen scaffold that had good biocompatibility for various skin regeneration associated cells. Because bFGF is a well-known factor for cell proliferation and vascularization, human bFGF gene was electrically transduced into human UC-MSCs, and the stable bFGF-overexpressing UC-MSCs (bFGF-MSCs) clones were screened out as seeding cells for wound healing. Then, the bFGF-overexpressing UC-MSCs were loaded onto a collagen scaffold to form a biomimetic skin material for accelerating full-thickness skin incision wound healing in a streptozotocin-induced diabetic rat model. Our novel collagen-based biomimetic skin scaffold combined of bFGF-MSCs successfully accelerated the diabetic skin wound healing *in vivo* via facilitating neovascularization, skin tissue formation, and re-epithelialization, indicating it would be a promising strategy for healing diabetic skin wounds and even other refractory tissue regenerations in clinic.

## MATERIALS AND METHODS

**Bioinspired Skin Collagen Scaffold Fabrication.** Bioinspired skin collagen scaffolds were mainly made of dermal collagen type I, prepared from bovine dermal collagen. Bovine skin tissue was submerged in a 0.5 M acetic acid solution for 8 h at 4 °C and then neutralized with 4 M NaOH. The resulting homogeneous solution was dialyzed in deionized water for 5 days. The dialyzed solution was then frozen at −80 °C for 24 h and subsequently lyophilized at −30 °C and 0.1 mbar until dry. The resultant porous collagen was sterilized using 25 kGy 60Co irradiation and stored at 4 °C until needed.

**Human MSCs Culture and Construction of Human bFGF Overexpressing MSCs (bFGF-MSCs).** This study was approved by the Committee on Human Research of Nanjing Drum Tower Hospital. Human MSCs were isolated from a 15 cm long fresh umbilical cord and

cultured according to a previously published protocol.<sup>17</sup> To construct bFGF-MSCs, the PCMV3 plasmid inserted with human bFGF DNA sequences was introduced into MSCs using an electroporator, and positive clones were selected using hygromycin at 100 ng/mL on the basis of our previous published study.<sup>18</sup> Clinical-grade MSCs were used for electroporation. We performed the electroporation using an optimized program in a CUY21EDIT II super multipulse *in vivo* and *in vitro* electroporator (BEX CO., Ltd.): pulse voltage (150 PpV), drive voltage (20 PdV), pulse time (10 ms), and number of cycles (20). The transfected cells were divided into two groups: blank control plasmid (NC) and recombinant bFGF plasmid. After electroporation, the mixture was inoculated into a 10 cm dish. After culturing at 37 °C and 5% CO<sub>2</sub> for 24 h, the cell status and mortality were observed, and then, 100 µg/mL hygromycin was used for stable clone screening. After 14 days, cell colonies were picked under a stereomicroscope (K-400L, MOTIC CHINA GROUP CO., Ltd.) for expansion culture, with each colony representing a cell line.

**Flow Cytometric Analysis.** For the assessment of surface marker expression in HUCMSCs and bFGF-HUCMSCs, cells were collected and  $1 \times 10^6$  cells per sample were incubated with antibodies conjugated to either fluorescein isothiocyanate (FITC) or phycoerythrin (PE). The antibodies used included CD34-FITC, CD45-FITC, CD90-FITC, CD19-PE, CD44-PE, CD73-PE, CD105-PE, and HLA-DR-PE (BD Biosciences, San Diego, CA, USA), and the incubation was carried out in the dark for 15 min. Subsequent to three washings with phosphate-buffered saline (PBS), the cells were analyzed using a FACScan flow cytometer (BD FACS Aria, NJ, USA) coupled with FlowJo V10 software, facilitating a detailed phenotypic characterization of the cells.

**Culture of Human Fibroblasts and Endothelial Cells.** The primary human skin fibroblasts (HFs) were extracted from human skin tissue sample according to our previously published literature<sup>19</sup> and were expanded when cells grew up about 90% of confluence. Then, the expanded HFs were cultured in high-glucose Dulbecco's modified eagle medium (DMEM) (Gibco) supplemented with 10% FBS. Human microvascular endothelial cells (ECs) obtained from the Cell Bank of the Chinese Academy of Sciences (Shanghai, China) were cultured and incubated at 37 °C, 5% CO<sub>2</sub> in DMEM medium (Gibco) containing 10% FBS, 1 µg/mL hydrocortisone (Sigma), 1% GlutaMAX (Gibco), and 10 ng/mL epidermal growth factor (Sigma).

**Property Evaluations of Bioinspired Collagen Scaffold.** The morphology of the collagen scaffold was observed by scanning electron microscopy (SEM) (GeminiSEM 500, Zeiss) after spraying with a thin gold layer. To investigate the biomimetic skin characteristics of the collagen scaffold, measurement of the surface contact angle and mechanical analysis were performed. Measurement of the surface contact angle on the scaffolds was determined using a contact angle system (KSV CAM-200, KSV Instruments). A high-speed camera, operating with a 2 ms frame interval, was utilized to capture the transient images of a 2 µL water droplet at the moment of impact on the surfaces. To analyze the mechanical feature of the collagen scaffold, the scaffold ribbons were positioned in a tensile testing device, after which the paper was removed (Lloyd TA500 Texture Analyzer with a 10 N load cell). The precise width and gauge length of the samples were measured by using digital calipers. The samples were subsequently stretched at a rate of 5 mm/min, while the load (in N) was monitored. Using this data, stress–strain plots were constructed. Strain (%) was calculated by dividing the elongation by the gauge length, whereas stress (MPa) was obtained by dividing the measured load by the surface area of the sample (width × thickness). The Young's modulus was determined from the slope of the linear region of the stress–strain curves.

**FTIR Test Analysis.** The prepared collagen scaffold was measured by using the IRSpirit Fourier transform infrared spectrometer. At room temperature, potassium bromide (KBr) was used as the background. Each sample's infrared spectrum signal was scanned 32 times. The testing frequency range was 4000 to 400 cm<sup>−1</sup>, with a resolution of 0.5 cm<sup>−1</sup>. Data processing, including absorbance/transmittance conversion and automatic smoothing, was performed by using OMNIC software. Data were peak-annotated using OMNIC 8.0, with baseline correction and normalization conducted prior to peak fitting. The Gauss Amp

function in PeakFit 4.12 was used for fitting the processed data. Spectra were plotted using the Origin 2017 software.

**Biocompatibility of the Collagen Scaffold.** A total number of  $5 \times 10^5$  green fluorescent protein (GFP)-overexpressing MSCs (GFP-MSCs) were seeded on the collagen scaffold to observe the proliferation of GFP-MSCs at 24, 48, and 72 h, respectively. To evaluate whether other important skin regeneration associated cells could also grow well on this material, GFP-MSCs were coinoculated with HF and ECs, respectively, and their proliferations were observed at different time points within 72 h under fluorescence microscope (Leica). EDU kit (R11053.8, RiboBio Co.Ltd.) was used to assay the proliferation of MSCs cultured in plate ( $5 \times 10^5$  cells per well) and on same acreage collagen scaffold ( $5 \times 10^5$  cells) according to the manufacture's instruction. Images were acquired with a fluorescence microscope. A Calcein-AM/PI double staining kit was used to assay the cell viability on collagen scaffold according to the manufacture's instruction. Then, simultaneous observations of live cells (green fluorescence) and dead cells (red fluorescence) were conducted using fluorescence microscopy.

**Collagen Scaffold's Binding Affinity and Sustained Release of bFGF.** Initially, we evaluated whether the collagen scaffold could effectively bind bFGF and, subsequently, sustain its release. The scaffold was immersed in a human bFGF protein solution at various concentrations for 12 h to facilitate binding. The bFGF concentration was assessed before and after binding to determine the quantity of the scaffold. bFGF loaded into the collagen scaffold was calculated by comparing bFGF concentration before and after loading as the following formula: Mass of loaded bFGF (pg) =  $(C_0 - C_t) \times V$ , where  $C_0$  represents the initial concentration of the bFGF solution,  $C_t$  is the concentration of the bFGF solution after 12 h loading, and  $V$  is the volume of the bFGF solution. Following this, the scaffold was immersed into 1 mL of PBS solution for the releasing test. The concentration of bFGF in the PBS was measured at predetermined intervals over 7 days to calculate the released bFGF amount, after which the scaffold was placed in fresh PBS every day for the next measurements. The formula for bFGF release amount is bFGF release amount =  $M_0 + M_v$ , where  $M_0$  is the mass of original loaded bFGF in the scaffold, and  $M_t$  is the mass of released GF in the PBS solution at time  $t$ .

Subsequently, a total number of  $1 \times 10^5$  MSCs were separately seeded in the 2 cm  $\times$  2 cm collagen scaffold and in a similarly sized well plate for 6 h. Then, the collagen scaffold was immersed into fresh basal medium. At predetermined time intervals of for 8 days, bFGF concentration in the basal medium solution was measured to calculate the released bFGF, and then, the sample was soaked into fresh basal medium solution for next measurement.

The ELISA kit for human bFGF (MultiSciences Biotech Co., Ltd.) was used to measure the bFGF concentration in this experiment, following the manufacturer's instructions. An automated enzyme immunoassay analyzer was used to measure the optical density (OD) at a wavelength of 450 nm.

**Cell Proliferation, Migration and Tube Formation Assay.** In our *in vitro* experiments with HF and ECs, we divided the setup into six groups, as follows: 1) Control group: consisting solely of basal medium solution, 2) Scaffold group: the scaffold was immersed in the basal medium solution, 3) MSCs group: MSCs were cultured with basal medium solution in six-well plates alone, 4) MSC+ scaffold group: MSCs were seeded onto a scaffold of the same size as the well plate with the addition of basal medium solution, 5) bFGF-MSCs group: bFGF-MSCs were cultured with basal medium solution in well plates alone, and 6) bFGF-MSCs scaffold group: bFGF-MSCs were seeded onto a scaffold of the same size as the well plate with the addition of basal medium solution.

In the above groupings, equal numbers of  $5 \times 10^5$  MSCs and bFGF-MSCs were cultured in each well/six-well plate and in collagen scaffolds of the same area as the six-well plate. After 48 h of incubation at 37°, supernatants were collected from each group and stored at -80° for future use.

The proliferation of HF and ECs in different groups was evaluated by an EDU kit (C10310-1, Guangzhou RiboBio Co., Ltd.) following the manufacturer's instructions. The transwell migration assay was performed to examine the migration of HF and ECs affected by

MSCs and bFGF-MSCs cultured on a bioinspired collagen scaffold. HF or ECs were seeded into the upper transwell inserts with conditioned medium harvested from MSCs or bFGF-MSCs on a culture dish or collagen scaffold. The HF or ECs could migrate across through upper transwell insert into bottom of below transwell, and the cell migration was analyzed by observing the number of traveled cells after 72 h culture under a microscope (Nikon). For tube formation assay, matrigel was put in a 48-well plate evenly at 4 °C, and a total of  $1 \times 10^4$  cells/well of ECs were seeded on the solidification matrigel. The tube formation was measured by an ImageJ instrument after 48 h.

**Establishment of Diabetic Skin Wound Model and Treatments in Rats.** Animal care and experimental procedures were approved by the Laboratory Animal Management Committee of Nanjing Drum Towel Hospital. Sprague-Dawley (SD) rats weighing about 200 g were chosen in this study. Intraperitoneal injection of streptozotocin (STZ; 60 mg/kg; Sigma), freshly dissolved in a 0.1 M phosphate-citrate buffer, was used to induce experimental diabetes in rats that had been fasted for 24 h. Blood glucose levels were monitored after 1 week, and rats showing blood glucose levels greater than 16.67 mM were selected as diabetic model rats for subsequent experiment. The diabetic rats were monitored for 2 weeks after the induction of skin wounds. Following the shaving of the anesthetized rats, two full-thickness excisional skin wounds, each measuring 14 mm in diameter, were created on the upper back of each rat. Then, the diabetic rats were randomly divided into six treatment groups: 1) PBS group (wounds treated with 200  $\mu$ L PBS), 2) Scaffold group (wounds covered by scaffold with 200  $\mu$ L PBS inoculated), 3) MSCs group (wounds treated with  $5 \times 10^5$  MSCs in 200  $\mu$ L PBS), 4) bFGF-MSCs group (wounds treated with  $5 \times 10^5$  bFGF-MSCs in 200  $\mu$ L PBS), 5) MSCs scaffold group (wounds covered by scaffold loaded with  $5 \times 10^5$  MSCs in 200  $\mu$ L PBS), and 6) bFGF-MSCs scaffold group (wounds covered by scaffold loaded with  $5 \times 10^5$  bFGF-MSCs in 200  $\mu$ L PBS). Briefly, the rats were subcutaneously injected with MSCs, bFGF-MSCs, and PBS around the wounds at 4 injection sites (50  $\mu$ L per site). On days 0, 7, 11, and 14 following surgery, the wounds were photographed and measured with calipers. The scaffold was removed approximately 2 weeks after application for subsequent experimental analysis. Fourteen days postoperation, the rats were euthanized, and skin samples were collected.

**Histopathology and Immunofluorescence Assays.** During the 2 weeks of wound healing treatment in rats, we continuously monitored the changes in the wounds. Skin tissue samples were collected on the seventh and 14th days of wound healing and were then paraffin-embedded and sectioned for subsequent use.

After skin samples isolation and fixation in paraformaldehyde, the tissues were embedded in paraffin for hematoxylin and eosin (H&E), masson, immunohistochemistry, and immunofluorescence stainings. The skin tissues were cut into 5  $\mu$ m-thickness sections for subsequently experiment. The primary antibodies were used as follows:  $\alpha$ -SMA (CST, 34105),  $K_i$ -67 (Abcam, ab16667), PCNA, and S100A4 (Abcam, ab124805).

For H&E staining, the skin tissue slices were fixed by 95% ethanol, followed by performing hematoxylin staining and then eosin solution staining. For Masson's trichrome staining, skin tissue sections were initially dewaxed with xylene and alcohol, followed by the subsequent steps in accordance with the Masson staining kit instructions (Baso, BA4079A). For immunofluorescence and immunohistochemistry staining, skin tissue sections were first deparaffinized, followed by antigen retrieval and then endogenous peroxidase removal with 3% hydrogen peroxide. Afterward, the slices were blocked with 5% FBS for 1 h at room temperature and then incubated with the antibody solution overnight at 4 °C in the first day. The next day, sections were washed in PBST and incubated with the corresponding secondary antibody at room temperature for 1 h. In immunofluorescence experiment, the skin sections were sealed by DAPI solution (Abcam, ab104139) after PBST washing and drying. Images were taken by confocal microscopy. In the immunohistochemistry experiment, a drop of DAB (Maxim, 2031) solution was applied to the sections and was stopped by water after microscopic observation. Hematoxylin was restained and then



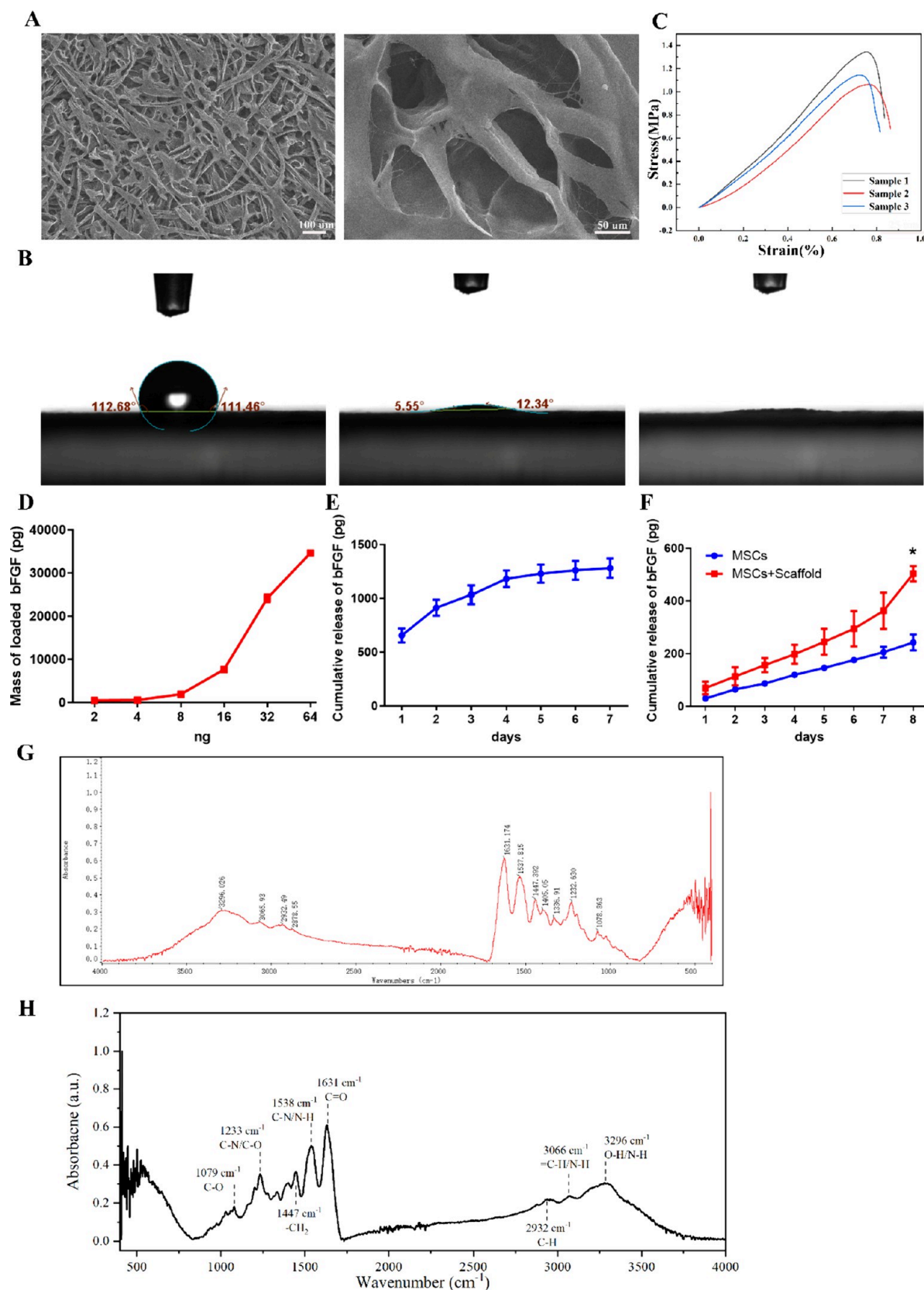


**Figure 1.** Structure and physicochemical properties of the bioinspired collagen scaffold. (A) SEM images showed the loose pores on the surface of bioinspired collagen scaffold. (B) Contact angle images of the bioinspired collagen scaffold. (C) The mechanical property of the bioinspired collagen scaffold. Samples 1, 2, and 3 represent three different piece of collagen scaffold, respectively. (D) The bFGF binding affinity of the bioinspired collagen scaffold with different concentrations of bFGF. (E) The bFGF's release curve of bioinspired collagen scaffold after saturated uptake of bFGF during 7 days. (F) The release curves of bFGF after MSCs were cultured on bioinspired collagen scaffold or dishes (\* $p < 0.05$ ). (G, H) The annotation and analysis of characteristic peaks in the infrared spectrum of collagen scaffold.

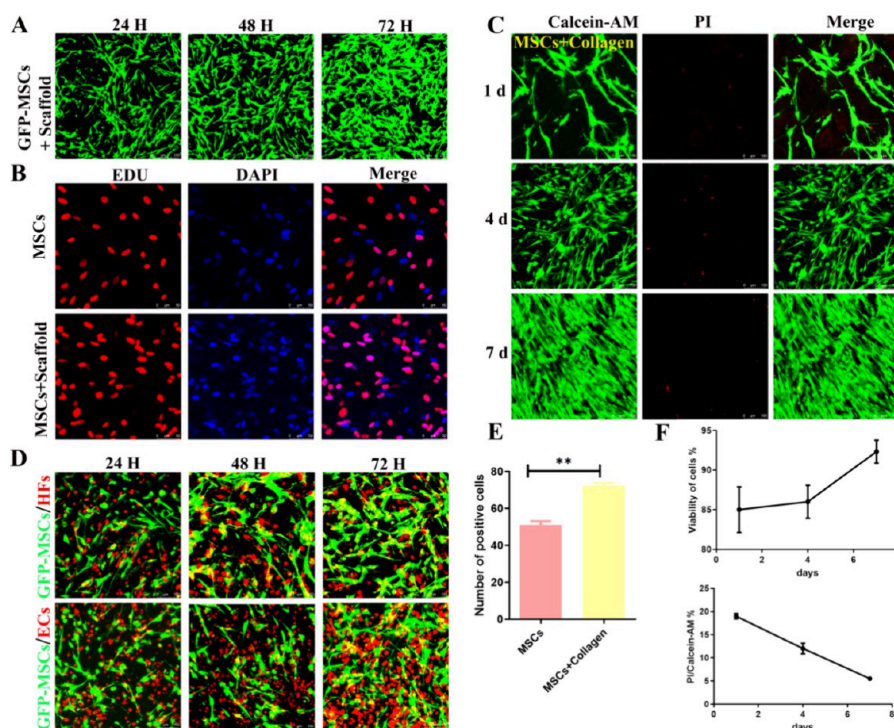


**Figure 2.** Cell biocompatibility of inspired collagen scaffold. (A) GFP-MSCs grew well and exhibited classic morphology of MSCs on inspired collagen scaffold. Scale bar = 250  $\mu\text{m}$ . (B) EDU assays showed MSCs had a better proliferation cultured on inspired collagen scaffold than them cultured on cover slides. Scale bar = 50  $\mu\text{m}$ . (C) The viability of MSCs on bioinspired collagen scaffold. The dead cells (PI positive staining) were less 99% of cells, indicating this material had little cytotoxicity for MSCs. Scale bar = 100  $\mu\text{m}$ . (D) GFP-MSCs (green) were cocultured with CD-Mil (red) labeled HFs or ECs on bioinspired collagen scaffold. Scale bar = 100  $\mu\text{m}$ . (E) The quantified proliferation rates of MSCs cultured on bioinspired collagen scaffold and culture dish by EDU analysis (\*\* $p < 0.01$ ). (F) The quantified viability of MSCs cultured on biomimetic skin scaffold and culture dish.

dehydrated with alcohol and permeabilized with xylene. Images were taken microscopically.

**Trace of CM-Dil-labeled UC-MSC *In Vivo*.** CM-Dil solution (2 mg/L) was added in UC-MSCs after digestion. The samples were incubated for 10 min at 37  $^{\circ}\text{C}$  and then for 15 min at 4  $^{\circ}\text{C}$ . Afterward, the labeled cells were examined for fluorescence using a microscope. Subsequently,  $5 \times 10^5$  labeled cells alone or loaded on collagen scaffold were transplanted into the wound site through subcutaneous injection. After retrieval of the skin wound in rat at day 10 after UC-MSCs transplantation, the skin tissues were embedded in paraffin and sectioned (5- $\mu\text{m}$  thick). Representative sections were stained with DAPI and costained with  $\alpha$ -SMA (CST, 3410S) and S100A4 (Abcam, ab124805) to examine the distribution and survival of the transplanted UC-MSCs *in vivo*. Images were taken by confocal microscopy.

**RNA Sequencing and Transcriptome Analysis.** RNA sequencing (RNA-seq) technology was utilized to explore the activation of angiogenesis and cell proliferation, related signaling pathways following bFGF introduction into MSCs. Total RNAs from MSCs and bFGF-MSCs were extracted and quantified using a NanoDrop device (Thermo Fisher Scientific). Libraries were prepared and sequenced on the Illumina HiSeq X Ten platform to generate 150 bp paired-end reads. The raw data (raw reads) were acquired in the FASTQ format through high-throughput sequencing and converted to original sequences via base calling. Data preprocessing, encompassing quantile normalization, was executed by using Trimmomatic software. The transcriptome sequencing and analysis were undertaken by OE Biotech (Shanghai, China). DESeq software was employed to identify differentially expressed genes (DEGs) based on fold changes and significance test results. DEGs were selected under the criteria of  $p$ -value  $< 0.05$  and fold change  $> 2$ . KEGG, a primary public database for pathway analysis, was used to examine the KEGG pathways of the DEGs. The enrichment of DEGs in each pathway was assessed using the hypergeometric test method, with a  $p$ -value  $< 0.05$  deemed statistically significant.

**Western Blot Assay.** MSCs and bFGF-MSCs were separately seeded onto the bioinspired collagen scaffold, followed by cultivation in basal medium solution after 6 h. Subsequently, the supernatants were collected 48 h postcultivation and then applied to serum-starved ECs. Protein from ECs was extracted at 0, 15 min, 30 min, 1 h, 3 h, and 6 h for Western blot analysis.

Cell lysates were prepared using a buffer containing protease inhibitors (Beyotime Biotechnology) following the manufacturers' protocols. Protein extraction was followed by concentration determination using a BCA Protein Assay Kit (Vazyme Biotech Co., Ltd.). Proteins were resolved through 10% SDS-PAGE and subsequently transferred onto PVDF membranes (Millipore). Membranes were then blocked with 5% BSA (Sigma-Aldrich) for 2 h and incubated with primary antibodies overnight at 4  $^{\circ}\text{C}$  on a horizontal shaker. On the subsequent day, the secondary antibody (1:10,000; Bioworld) was applied for 1 h at room temperature. Primary antibodies employed included anti-GAPDH (1:50,000; Proteintech, Wuhan, China), anti-SMAD2 (1:1000; Beyotime), antiphospho-SMAD2 (1:1000; Beyotime), anti-AKT (1:1000; ab179463, Abcam), antiphospho-AKT (1:1000; ab81283, Abcam), anti-ERK1/2 (1:2000; Proteintech), antiphospho-ERK1/2 (1:1000; Beyotime), anti-HIF-1 $\alpha$  (1:1000; ab179483, Abcam), and anti-HIF-1 $\beta$  (1:1000; ab270520, Abcam).

**Statistical Analysis.** For each experiment, at least three replicates of each data set were expressed as the mean  $\pm$  standard deviation (SD). The data were subsequently presented and analyzed using one-way ANOVA with Tukey's multiple comparison test via GraphPad Prism version 5.0. A  $p$ -value of less than 0.05 was deemed statistically significant.

## RESULTS

**Characterization of Bioinspired Collagen Scaffold.** The bioinspired collagen scaffold exhibited porous structures on its surface under SEM, and the diameters of loose pores were about 10–50  $\mu\text{m}$  (Figure 1A). To assay the surface hydrophilicity of



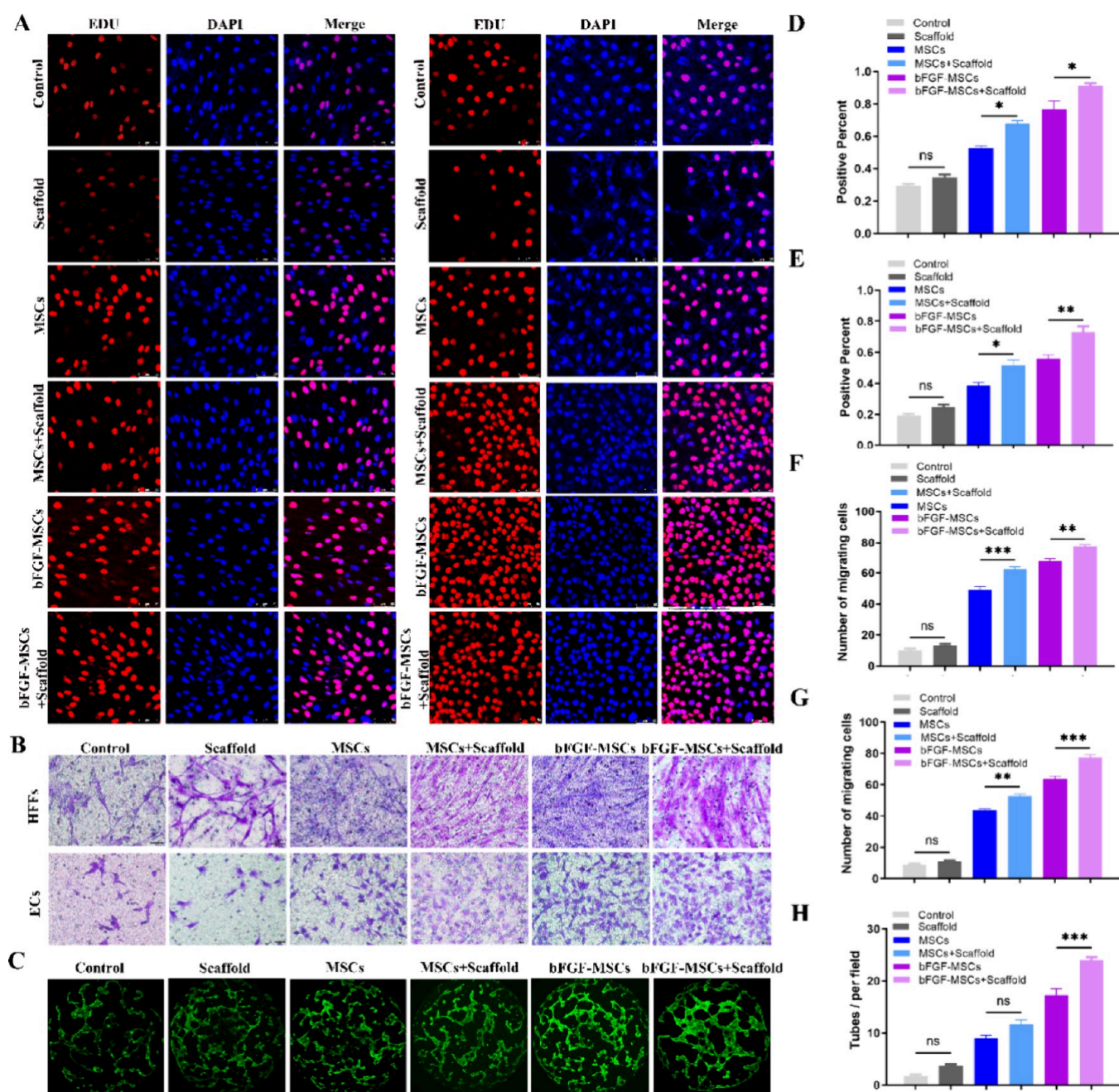


**Figure 3.** MSCs and bFGF-MSCs cultured on collagen scaffold enhanced the migration, proliferation, and angiogenesis of HFs and ECs. (A, D, E) Representative images and quantified data of proliferations of HFs and ECs under different treatments were tested by EDU analysis. Scale bar = 50  $\mu$ m. (B, F, G) Representative images and quantified data of migrations of HFs and ECs were stimulated by conditioned mediums from MSCs and bFGF-MSCs cultured on dishes or bioinspired collagen scaffold by the transwell assay. Scale bar = 100  $\mu$ m. (C, H) Representative images and quantified data of the tube formation of ECs on matrigel under different treatments. Scale bar = 200  $\mu$ m. \* $p$  < 0.05, \*\* $p$  < 0.01, \*\*\* $p$  < 0.001.

the bioinspired collagen scaffold, surface contact angles of water droplets collided on the collagen scaffold were determined using a contact angle system. The results showed the contact angles of collided water droplets on material were 111–112°, 5–12°, and 0° along with time, respectively, suggesting the bioinspired collagen scaffold had a good hydrophilic property to absorb exudate and maintain moisture around the wound area where it was applied to cover skin injured site (Figure 1B). The mechanical property assay showed that the bioinspired collagen scaffold also had adaptive tensile capacity of withstanding stretching compared with the rat skin fibers (Figure 1C).

The ELISA method was employed to assess the binding capability and release rate of the bioinspired collagen scaffold for the cytokine bFGF, as well as to quantify the release of bFGF following MSCs incubation with or without the scaffold. As depicted in Figure 1D, there was a proportional increase in the amount of bFGF bound to the scaffold with rising concentrations of exogenously added bFGF, demonstrating the scaffold had intrinsic binding affinity of bFGF. Subsequently, after they had absorbed a sufficient quantity of bFGF, the daily bFGF release rate of bioinspired collagen scaffold after saturated absorption was measured over the course of a week. It was observed that bFGF was gradually released throughout the



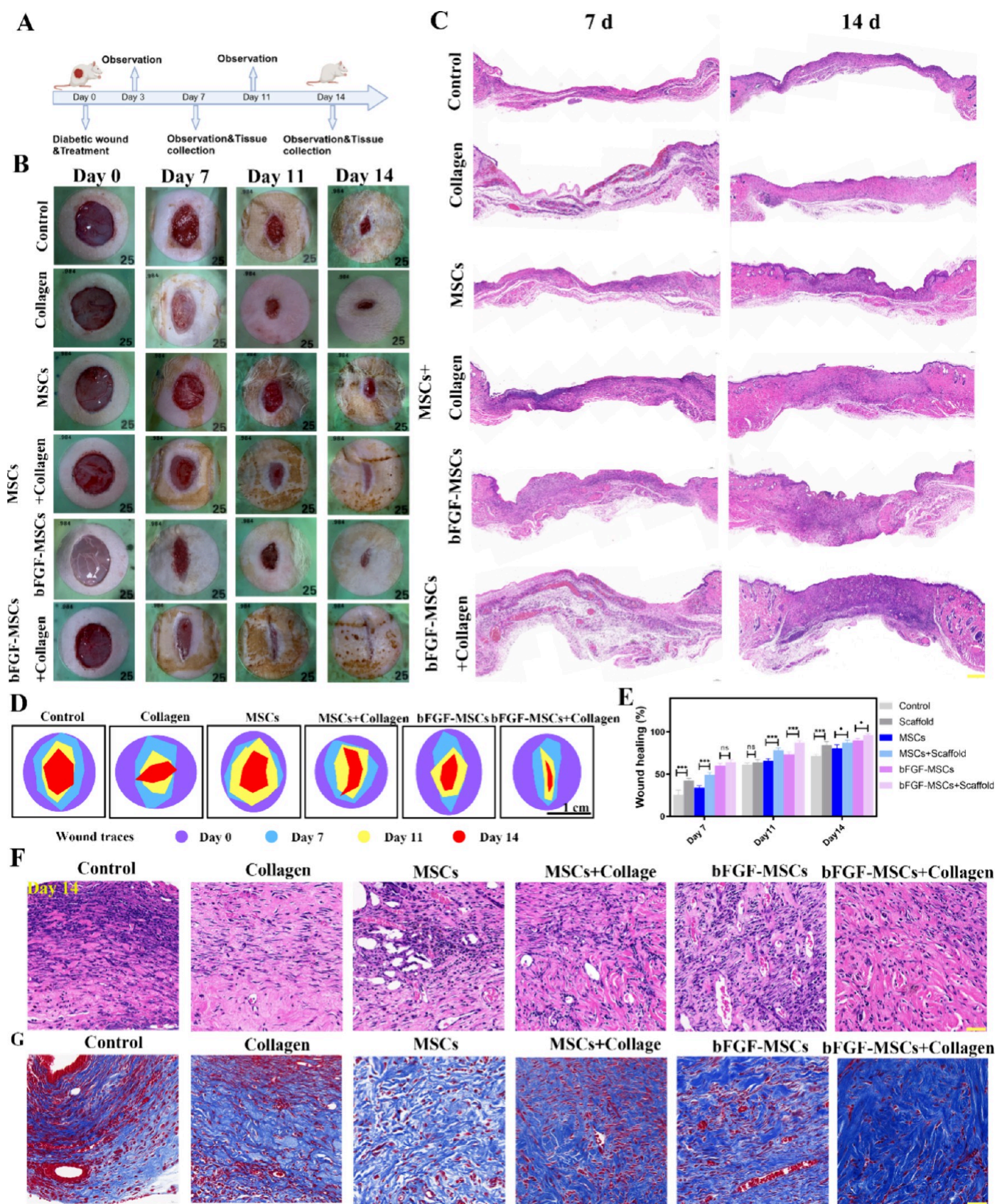


**Figure 4.** Bioinspired collagen scaffold loaded with MSCs/bFGF-MSCs accelerating rat diabetic skin wound healing. (A) Flowchart of experimental procedures. (B) Representative images of skin wound healings after different treatments at indicated time points. (C) H&E staining images of wound samples at days 7 and 14 (scale bar = 500  $\mu\text{m}$ ). (D) Schematic images of wound-bed closure during 14 days *in vivo* of treatment with different formulations. (E) Quantification of wound-healing data from rats *in vivo* wound recovery with different strategies (\* $p < 0.05$ , \*\*\* $p < 0.001$ ). (F) The magnified H&E staining images at wound sites in all groups at day 14 (scale bar = 40  $\mu\text{m}$ ). (G) Masson's trichrome stainings of wound sample sections in all groups (scale bar = 40  $\mu\text{m}$ ).

week, with a stable concentration of bFGF after 5 days (Figure 1E). Interestingly, the same amount of MSCs cultured on the scaffold could secrete higher bFGF into the medium than those cultured in the dish (Figure 1F). The collagen scaffold was measured using the IR Spirit Fourier transform infrared (FTIR) spectrometer. Figure 1G shows the infrared characteristic peaks of the collagen material, with an analysis of its infrared absorption peaks. Figure 1H illustrates the functional group composition and major components of the collagen material.

#### Biocompatibility of the Bioinspired Collagen Scaffold.

The good biocompatibility of the regenerative materials is important to heal severe skin wound lesions. We planned to use bioinspired collagen scaffold loaded with MSCs to cure diabetic skin damage, and we first investigated the biocompatibility of the bioinspired collagen scaffold for MSCs. GFP-overexpressing MSCs (GFP-MSCs) were seeded on this material, and their growth was observed under fluorescence microscopy at 24, 48, and 72 h, respectively. GFP-MSCs could tightly adhere and grow well on collagen scaffold along with the time (Figure 2A). An EDU assay also confirmed that MSCs on a bioinspired collagen scaffold had a better proliferation rate compared with MSCs on culture slides (Figure 2B and E). Then, Calcein-AM/PI staining was performed to assay the viability of MSCs on bioinspired collagen scaffold, and the cell viability is over 90% at all indicated time points, indicating this collagen scaffold had no cytotoxicity for MSCs (Figure 2C and F). When GFP-MSCs were cocultured with other skin cell HFs and ECs on bioinspired collagen scaffold, respectively, both HFs and ECs showed good growth on this material (Figure 2D).

**Bioinspired Collagen Scaffold Loaded with bFGF-MSCs Promoting the Migration, Proliferation, and *In Vitro* Angiogenesis of HFs and ECs.** We transfected MSCs with a bFGF plasmid containing the IL2 signal peptide and subsequently screened out ten different clonal strains (Figure S1). The concentrations of secreted bFGF in the supernatant of these stable strains were measured using a corresponding ELISA kit. The number 4 clone of bFGF-MSCs, which exhibited the highest expression level of bFGF, was selected for further expansion and subsequent experiments. The surface markers of selected bFGF-MSCs were characterized by using flow cytometry sorting techniques (Figure S2). The bFGF-MSCs met the surface marker criteria of the MSCs.

The skin regeneration is involved in a variety of skin associated with cells, including HFs and ECs. Their proliferation and migration play important roles in diabetic wound healing processes. Then, we investigated the effects of bFGF-MSCs on HFs and ECs. EDU analysis was applied to measure the proliferation of HFs and ECs upon stimulation of condition mediums from MSCs and bFGF-MSCs on an inspired collagen scaffold (Figure 3A). The results showed that the proliferations of HFs and ECs were markedly increased in response to conditioned medium from cultured MSCs and bFGF-MSCs in dishes compared to control and alone inspired collagen scaffold groups. MSCs and bFGF-MSCs cultured on a collagen scaffold induced higher increases in proliferation than those cultured on dishes. Among all groups, condition medium from bFGF-MSCs cultured on a collagen scaffold had the best stimulation on proliferations of HFs and ECs (Figure 3D–E). MSCs or bFGF-MSCs cultured on a collagen scaffold could markedly enhance the migrations of HFs and ECs, compared with those cultured on dishes (Figure 3B). In addition, the bFGF-MSCs groups had better migrations of HFs and ECs compared with MSCs groups (Figure 3F–G). Then, the effect of bFGF-MSCs on angiogenic

activity of ECs was assessed by the tube formation assay on the matrigel. As shown in Figure 3C, ECs on matrigel were cultured with condition medium harvested from MSCs and bFGF-MSCs on culture dish or bioinspired collagen scaffold. Results showed that MSCs or bFGF-MSCs improved more formations of capillary-like structures of ECs compared to the control and scaffold groups. Quantitative measurements revealed that bFGF-MSCs cultured on bioinspired collagen scaffold had the best stimulation on tube formation including tube length and number among all groups (Figure 3H). These data confirmed that our inspired collagen scaffold was a good material for bFGF-MSCs to facilitate the regenerative characteristics of skin cells.

#### Bioinspired Collagen Scaffold Loaded with MSCs or bFGF-MSCs Accelerating Diabetic Wound Healing in Rats.

The healing of severe chronic skin wounds in diabetic patients is involved with complex regeneration processes. Therefore, the combination of a bioinspired collagen scaffold and seeding cells would be favorable for diabetic wound healing. Therefore, the bioinspired collagen scaffolds loaded with MSCs/bFGF-MSCs were applied to repair the diabetic full-thickness excision skin wound in rats. Rat experimental diabetes was induced by intraperitoneal injection of STZ. Blood glucose levels were markedly increased after 1 week (Figure S3), and the rats with blood glucose level greater than 16.67 mM were selected as diabetic model rats for subsequent experiments. The wound-healing potential of the collagen scaffold was evaluated *in vivo* using a full-thickness skin defect model in diabetic rats (Figure 4A). The diabetic rats were carried out with two full-thickness excisional skin wounds (14 mm in diameter) on the upper back of each rat after shaving the anaesthetization. The gross images of diabetic skin wounds after different treatments showed that the wound areas in all groups were obviously reduced after treatments at day 7, and the wounds in the bioinspired collagen scaffold loaded with MSCs or bFGF-MSCs groups were basically covered with newly formed skin tissue (Figure 4B). Among all groups, a bioinspired kin collagen scaffold loaded with bFGF-MSCs had the fastest healing (Figure 4D, E). H&E staining showed bioinspired collagen scaffolds loaded with MSCs or bFGF-MSCs have much thicker newly formed epidermis and dermis with hair follicles and fat cells in wound sites (Figure 4C). Figure 4E presents the quantitative analysis of wound healing percentages at various time points (days 7, 11, and 14). It demonstrated that the bFGF-MSCs + Scaffold group had the highest wound healing percentage, indicating the most effective treatment. Noticeably, the bioinspired scaffold loaded with bFGF-MSCs had the best re-epithelialization, having more skin appendages and newly formed blood vessels in wound sites compared with other treatment groups at day 14 (Figure 4F). The alone bioinspired collagen scaffold only slightly promoted skin wound healing compared with the model group. In addition, Masson's trichrome staining was performed to exhibit the collagen deposition in the wound sites after different treatments (Figure 4G). At day 14 postoperation, few collagen fibers were observed in the control group. The bioinspired collagen scaffold loaded with MSCs or bFGF-MSCs group showed much more collagen deposits in wound sites than corresponding alone MSCs or the bFGF-MSCs group. Among them, bioinspired collagen scaffold loaded with bFGF-MSCs treatment led to the highest amount of collagen deposits in wound sites. Together, these results of H&E and Masson stainings revealed that the bioinspired collagen scaffold loaded with bFGF-MSCs had the best therapeutic outcomes for diabetic wound healing, including enhancing the



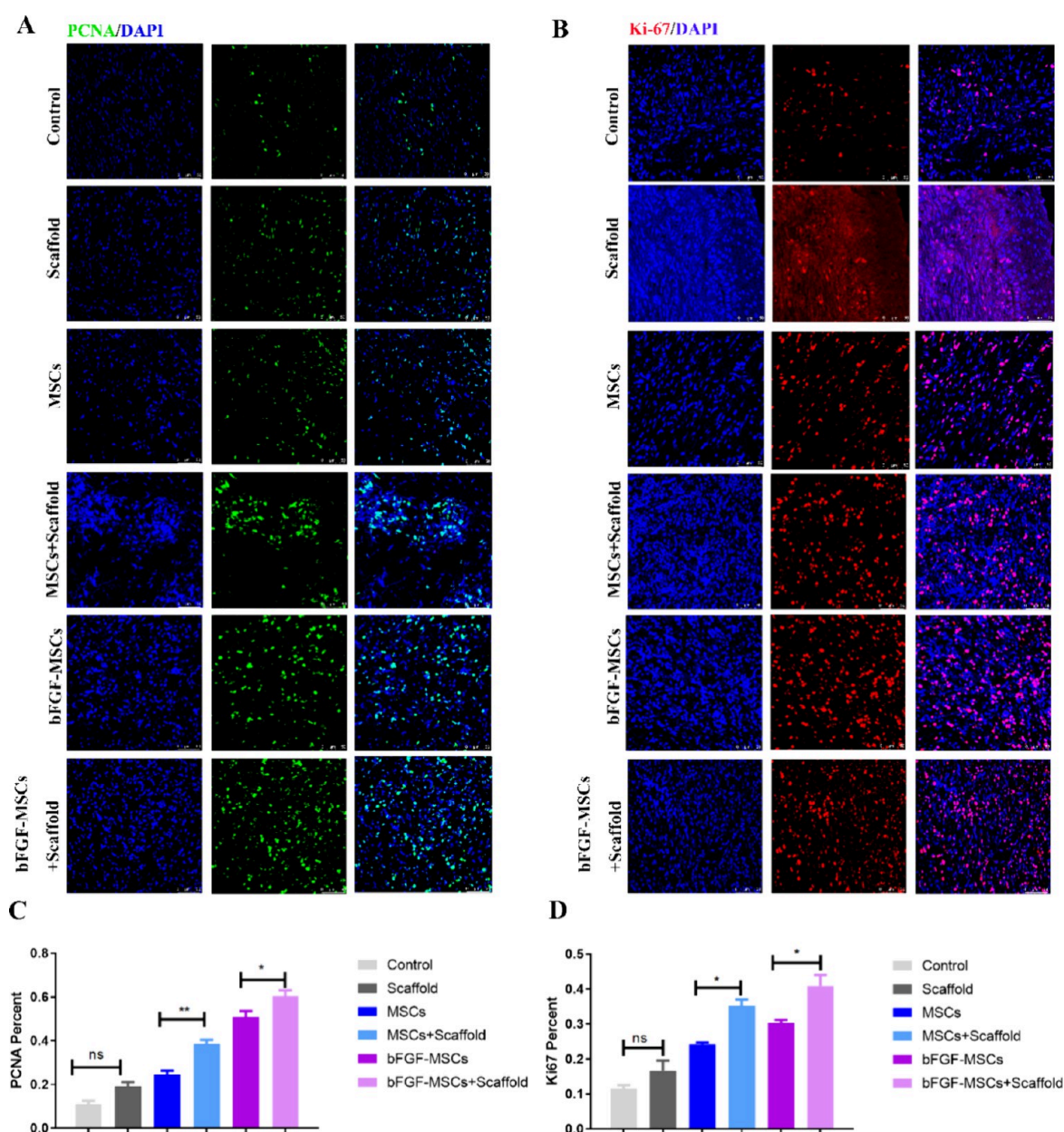


**Figure 5.** Proliferations of skin cells at injured sites by PCNA and  $K_i$ -67 stainings post different treatments. (A, B) Representative images of PCNA and  $K_i$ -67 stainings in wound sample sections (scale bar = 50  $\mu$ m). (C, D) Quantification of PCNA and  $K_i$ -67-positive skin cells in wound sections. \* $p$  < 0.05, \*\* $p$  < 0.01, and \*\*\* $p$  < 0.001.

formation of granulation tissue and collagen production, and eventually accelerating diabetic skin wound healing process.

**Bioinspired Collagen Scaffold Combined with bFGF-MSCs Promoting the Proliferation of Skin Cells in Diabetic Wound Healing.** PCNA and KI-67 are markers of cell proliferation. Immunostainings with antibodies against PCNA and KI-67 were performed to investigate the effect of inspired collagen scaffold combined with MSCs or bFGF-MSCs on the proliferation of skin cells in diabetic wound healing (Figure 5). On the whole, the result of PCNA staining was consistent with  $K_i$ -67 staining. There were a small number of PCNA and  $K_i$ -67 positive skin cells in the control and alone collagen scaffold groups in wound sites. Except from these two groups, all of the other groups had strong positive stainings of PCNA and  $K_i$ -67 in wound sites. The alone bFGF-MSCs treatment had better proliferation staining than the alone MSCs treatment.

Obviously, the bioinspired collagen scaffold loaded MSCs or bFGF-MSCs group had significantly higher number of PCNA and  $K_i$ -67 positive cells, compared with corresponding alone MSCs or bFGF-MSCs group. Especially the bioinspired collagen scaffold loaded bFGF-MSCs group had the best promotion of skin cells' proliferation among all groups, potentially contributing to faster and better diabetic wound healing than other treatments

**Bioinspired Collagen Scaffold Combined of MSCs/bFGF-MSCs Boosting the Angiogenesis in Diabetic Wound Healing.** Terminal vascular damage is one of the serious complications of diabetes mellitus, and neovascularization is essential for diabetic skin regeneration. The  $\alpha$ -smooth muscle acting ( $\alpha$ -SMA) is a marker of blood vessels. Thus, the  $\alpha$ -SMA staining of wound sections was performed to investigate whether bioinspired collagen scaffold loading MSCs or bFGF-

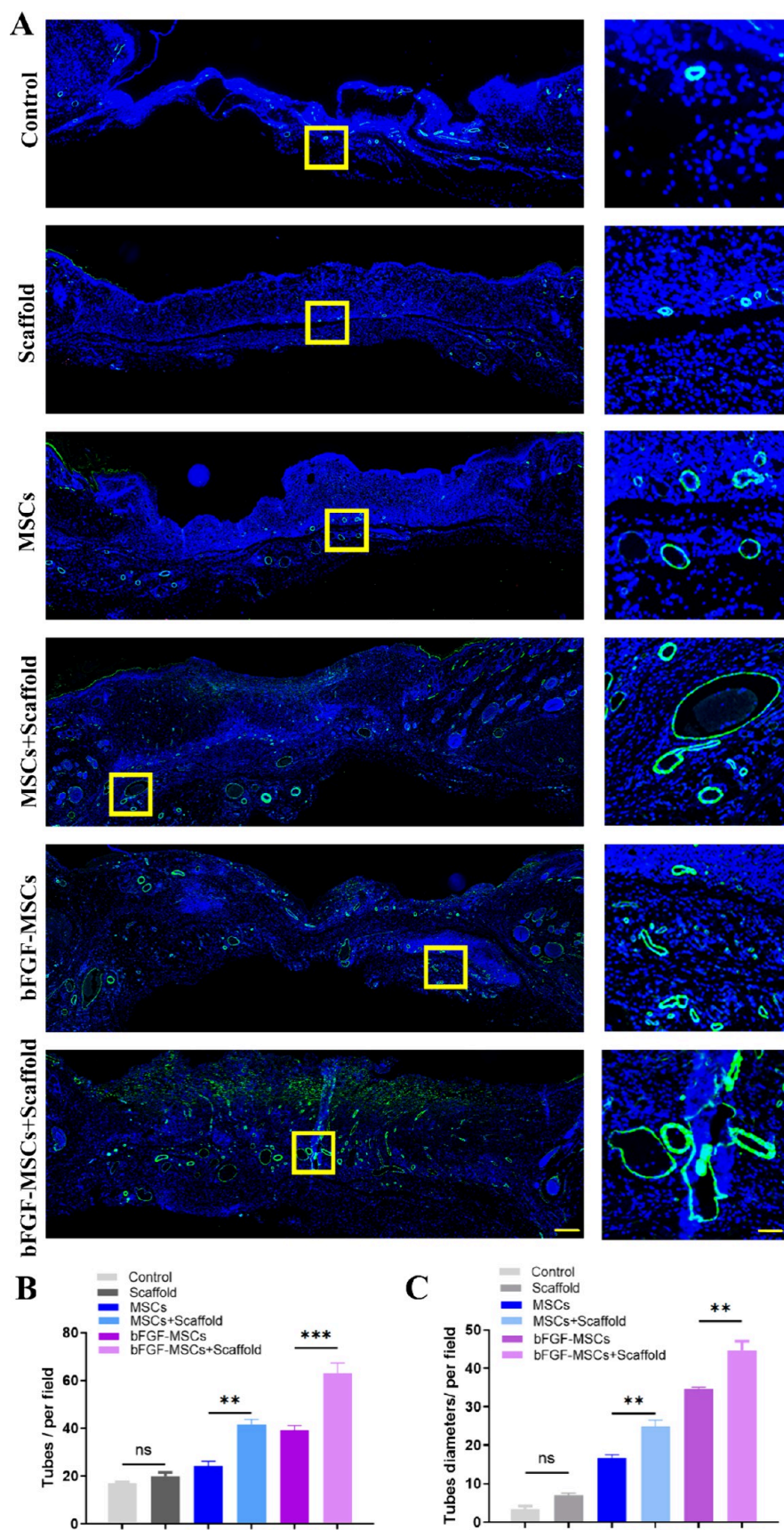


**Figure 6.**  $\alpha$ -SMA immunostainings of skin wound samples post different treatments. (A) Representative  $\alpha$ -SMA immunostaining images of skin wound sections (right panel, bar scale = 200  $\mu$ m; left panel, bar scale bar = 50  $\mu$ m). (B) Quantified data of newly formed blood vessels in different groups. \* $p < 0.05$ , \*\* $p < 0.01$  and \*\*\* $p < 0.001$ . (C) Diameters of newly formed blood vessels in different groups. \* $p < 0.05$ , \*\* $p < 0.01$  and \*\*\* $p < 0.001$ .



MSCs could enhance the angiogenic responses during diabetic wound healing. As shown in Figure 6A, very few  $\alpha$ -SMA positive cells were observed in the control and alone bioinspired collagen scaffold groups. MSCs or bFGF-MSCs treatment improved the  $\alpha$ -SMA staining, but bioinspired collagen scaffold loading MSCs or bFGF-MSCs remarkably boosted positive stainings of  $\alpha$ -SMA compared with alone the corresponding cell treatment. Among all groups, bioinspired collagen scaffold loading bFGF-MSCs was able to maximize the promotion of neovascularization, including the number and tube diameter of newly formed blood vessels in wound sites. These results indicated that our bioinspired collagen scaffold could facilitate MSCs or bFGF-MSCs to efficiently boost the angiogenesis in diabetic skin wound *in vivo* (Figure 6B, C).

**Distribution and Fate of Transplanted MSCs on Bioinspired Collagen Scaffold in Wound Sites.** To trace the transplanted MSCs *in vivo* after treating the skin wound, CM-Dil (red) labeled MSCs (CM-Dil-labeled MSCs) (red) were transplanted into the diabetic skin wound by peripheral diffusion injection or a bioinspired collagen scaffold incubation method. At day 10 post transplantation, the injected CM-Dil-labeled MSCs were concentrated in a shallow layer of the skin at the injected sites, while CM-Dil-MSCs seeded on a bioinspired collagen scaffold could infiltrate into deep skin tissues and evenly distribute over the entire wound site (Figure 7A). Afterward, we investigated whether the transplanted MSCs could differentiate into vascular-related cells or skin fibroblasts. The  $\alpha$ -SMA immunostaining showed that CM-Dil-labeled MSCs did not overlap the positive  $\alpha$ -SMA cells. Similarly, S100A4 (a marker of skin fibroblasts) staining also showed CM-Dil-labeled MSCs did not colocalize S100A4 positive cells (Figure 7B). These results clearly indicated that transplanted CM-Dil-labeled MSCs did not differentiate into vascular-related cells or skin fibroblasts *in vivo*, suggesting that the mechanism by which MSCs enhanced diabetic skin wound healing was not through direct differentiations of skin-associated cells but through paracrine action.

**Mechanism Pathways of bFGF-MSCs in Promoting Diabetic Skin Wound Healing.** The above results confirmed that bFGF-MSCs could significantly accelerate diabetic skin wound healing through newly formed blood vessels. Then, we further investigated the mechanism by which bFGF-MSCs promoted the neovascularization in diabetic skin wound healing. The RNA-Seq assay was utilized to screen differential biological processes between MSCs and bFGF-MSCs, which were enriched with differentially expressed genes. Further analysis of several pathways revealed major changes linked to angiogenesis. The results were statistically significant and were transformed into KEGG and GO maps. These findings suggest that overexpressing bFGF in MSCs could potentially enhance the capacity of endothelial cells (ECs) to perform angiogenesis at the skin injured sites. The AKT-HIF1 signal pathway is vital for skin wound healing. To demonstrate this point, we initially collected the culture supernatants of MSCs or bFGF-MSCs after a 48 h incubation on bioinspired collagen scaffold using basal medium. ECs were starved using basal medium without FBS for 12 h and then cultured with the above condition medium. ECs were harvested following stimulation at 0, 15, 30, 60, 180, and 360 min for Western blot analysis. The results indicated a lasting high level of AKT phosphorylation and an increase in HIF-1 $\alpha$  and HIF-1 $\beta$  protein levels after stimulation of condition medium from bFGF-MSCs, suggesting bFGF-MSCs may better enhance the angiogenic capability of ECs by activating HIF-1 signal pathway in diabetic skin wound

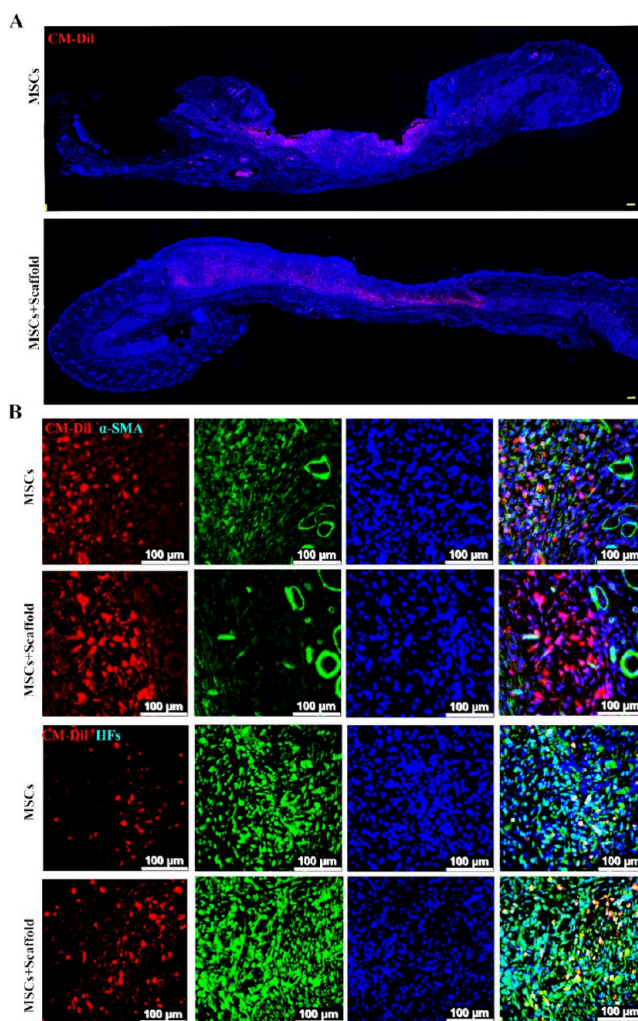


**Figure 7.** Tracing the transplanted CM-Dil-labeled MSCs *in vivo*. (A) Representative images of CM-Dil-labeled MSCs at skin wound after transplantation (blue, DAPI staining of the nucleus; red, CM-Dil-labeled MSCs; scale bar = 100  $\mu$ m). (B) Representative images of  $\alpha$ -SMA or S100A4 immunostaining and CM-Dil-labeled MSCs at the wound sites (scale bar = 100  $\mu$ m).

healing. As illustrated in Figure 8D, immunohistochemical stainings for HIF-1 $\beta$  and VEGFA demonstrated minimal expression levels in both in control and alone bioinspired collagen scaffold groups. MSCs or bFGF-MSCs treatment improved the expression of HIF-1 $\beta$  and VEGFA stainings, but bioinspired collagen scaffold loading MSCs or bFGF-MSCs remarkably boosted positive stainings of HIF-1 $\beta$  and VEGFA in sections of skin wound samples compared with the alone corresponding cell treatment. These results indicated that the bioinspired collagen scaffold synergistically enhances the pro-angiogenic potential of MSCs or bFGF-MSCs in diabetic skin wound healing *in vivo*.

## DISCUSSION

There have been many attempts to accelerate the nonhealing diabetic wounds, but the optimal treatment strategy is still being researched.<sup>20</sup> The objective of this study was to fabricate a type of bioinspired collagen scaffold to loaded bFGF-MSCs for covering severe skin wounds in diabetic patients with the aim of continuously releasing bFGF to enhance wound healing. We found that this collagen-based scaffold had excellent biocompat-

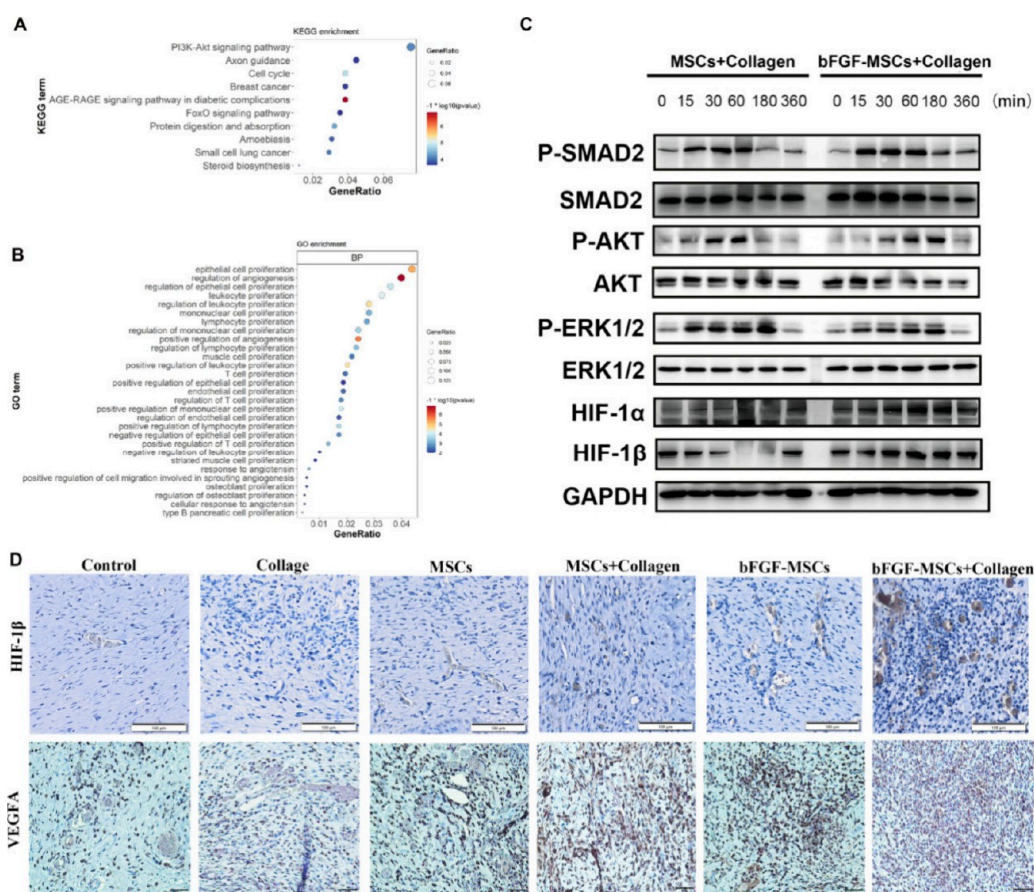


**Figure 8.** Activation of AKT-HIF1 signal pathway by bFGF-MSCs. (A, B) KEGG and GO maps of differentially expressed genes between MSCs and bFGF-MSCs. (C) Western blot analysis of SMAD2, AKT, ERK1/2, HIF-1 $\alpha$ , and HIF-1 $\beta$  protein levels in ECs treated with condition medium from MSCs or bFGF-MSCs at the indicated time points (0, 15, 30, 60, 180, and 360 min). (D) Representative HIF-1 $\beta$  and VEGFA histological staining images of skin wound sections (scale bar = 100  $\mu$ m).

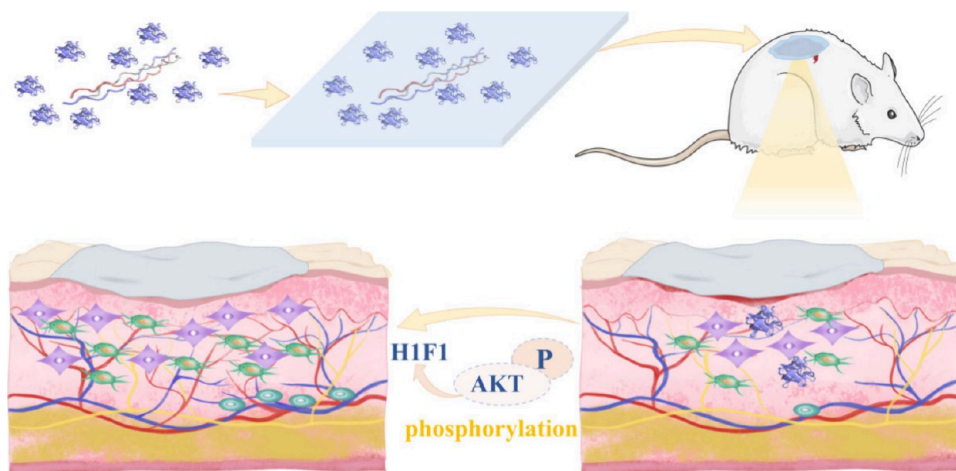


**Figure 9.** Illustration of biomimetic collagen scaffold loaded with bFGF-MSCs for sustained-release of bFGF for accelerating skin diabetic wound healing.

ibility and supported bFGF-MSCs to facilitate the migration and proliferation of HFs and ECs, as well as the tube formation of ECs *in vitro*. Moreover, the biomimetic skin collagen scaffold loaded with bFGF-MSCs also excellently promoted cellular proliferation and angiogenesis in skin wounds, contributing to neovascularization, collagen synthesis, and skin remodeling, collectively accelerating the healing of diabetic wounds *in vivo*. Additionally, it was observed that the bioinspired collagen

scaffold loading bFGF-MSCs significantly enhanced therapeutic outcomes in diabetic wound healing by promoting neovascularization of ECs through AKT-HIF-1 signaling pathway activation. The schematic diagram is shown in Figure 9.

Previous studies had shown that MSCs treatment was helpful for diabetic wound healing through activating various signal pathways.<sup>21–23</sup> Traditionally, MSCs have been administered via subcutaneous and intramuscular transplantation, or combined



with hydrogel scaffolds, to treat diabetic wounds.<sup>24,25</sup> To our knowledge, direct injection of MSCs had been deemed unsatisfactory for promoting repair because of the rapid leakage from the wound site and the decreased survival rate of transplanted MSCs due to the poor microenvironment.<sup>23,26,27</sup> To avoid these limitations, we successfully developed a novel collagen-based biomimetic scaffold, which was suitable for skin injury repair with many advantages over the currently used soft gel materials, including good water absorption, mechanical properties, and excellent biocompatibility. Our collagen biomimetic scaffolds were able to support good proliferation for various types of cells such as MSCs, HFs, and ECs, with little apoptosis.

bFGF is a potent mitogen for fibroblasts and keratinocytes and plays a significant role in wound healing and tissue repair. Previous reviews had summarized that the low levels of bFGF activity at the wound site would be detrimental to the diabetic skin wounds.<sup>28</sup> The application of bFGF protein could accelerate skin wound healing by promoting neovascularization, collagen deposition, and re-epithelialization. However, bFGF protein has a very short half-life *in vivo*, limiting its efficacy in clinical applications when administered locally or systemically.<sup>29,30</sup> To address these limitations of bFGF therapy, we established a stable bFGF-MSCs strain which was already verified to meet the standards and safety requirements of clinic-grade MSCs for clinical use, as demonstrated in our previous study.<sup>18</sup> Specifically, we performed systematic evaluations including assessments of the morphology, surface marker expression, differentiation potential, karyotype stability, and tumorigenicity. The study confirmed that bFGF-overexpressing MSCs did not induce tumor formation in nude mice and did not activate tumor-associated signaling pathways. Interestingly, exogenously administered bFGF showed dose-dependent binding to our bioinspired collagen scaffold, followed by a gradual release over the subsequent days. This suggested that the collagen scaffold could not only provide a carrier for bFGF-MSCs but also prolong the half-life of bFGF secreted by bFGF-MSCs. Additionally, we also observed that MSCs cultured on a bioinspired collagen scaffold could secrete higher bFGF protein than cultured in dishes. In previous studies, some researchers have fused a collagen-binding domain (CBD) with bFGF to improve the sustained release of growth factors in collagen materials, thereby enhancing angiogenesis and wound healing.<sup>31</sup> Compared with the CBD fusion method, using bFGF-MSCs offers several potential advantages. MSCs can serve as vehicles for targeted delivery of growth factors, enabling localized and sustained release directly at the wound site. This cell therapy approach can enhance the bioavailability and therapeutic effects of bFGF. Moreover, MSCs provide additional therapeutic benefits beyond the release of bFGF, including immunomodulation, secretion of other regenerative cytokines, and the ability to differentiate into various cell types, all of which contribute to improved wound healing. Additionally, MSCs can dynamically interact with the wound microenvironment, responding to signals, and potentially enhancing regeneration. These dynamic interactions and multifaceted therapeutic benefits underscore the potential of bFGF-MSCs to significantly improve wound healing outcomes compared with static delivery systems such as CBD fusion.

Diabetic wound healing is a complex process that involves numerous cells, growth factors, and the extracellular matrix.<sup>32,33</sup> Impairment of wound healing is a common issue among diabetic patients, often accompanied by infections, diabetic angiopathy,

and oxidative damage, which can lead to persistent ulceration. In this study, we used STZ-induced animal models, which are a widely used model for studying diabetic wound healing, to establish a rat model of type 1 diabetes mellitus.<sup>34</sup> The bioinspired collagen scaffold loading MSCs or bFGF-MSCs like a artificial skin were covered the diabetic skin wound, and this approach could reduce microbiological contamination at wound sites and promote the transplanted cells to infiltrate deep skin tissue. Overall, bFGF-MSCs treatment had better therapeutic outcomes for diabetic skin wounds compared with MSCs treatment. Furthermore, bioinspired collagen scaffold loading MSCs or bFGF-MSCs markedly accelerated diabetic skin wound healing compared with the corresponding alone cell treatment group. Especially, bioinspired collagen scaffold loading bFGF-MSCs had the best recovery of diabetic skin wounds among all groups, including the highest degree of granulation tissue formation, angiogenesis, and collagen deposition. The scaffold group loaded with bFGF-MSCs exhibited the highest levels of both indicators. These results proved that our research objectives have been fully achieved.

The healing of diabetic skin wounds is attributed to multiple factors such as skin cell proliferation, with niche improvement, extracellular matrix deposit, and tissue remodeling. The myofibroblast marker ( $\alpha$ -smooth muscle actin)  $\alpha$ -SMA represents dermal microvessels and mature vascularization.<sup>35</sup> Angiogenesis, the generation of new blood vessels, is essential for the repair of diabetic wounds.<sup>36–38</sup> A deficiency in angiogenesis is believed to be a major factor contributing to the delayed healing of diabetic wounds.<sup>39</sup> In this study, the density of positive  $\alpha$ -SMA staining was highest at skin wounds in the bioinspired collagen scaffold loading bFGF-MSCs group among all groups. Thus, it is noteworthy that our bioinspired collagen scaffold loading bFGF-MSCs were able to maximize the formation of neovascularization, including the number and tube diameter of newly formed blood vessels in wound sites. *In vitro*, the condition medium from bFGF-MSCs also markedly promoted the proliferation and tube formation of ECs. Generally, the proliferation of ECs represents the initial stage of angiogenesis which was then followed by the migration, adhesion, and differentiation of ECs.<sup>40</sup> Thus, the enhanced formation of new blood vessels in bioinspired collagen scaffold loading bFGF-MSCs may be the most important factor in diabetic skin wound healing.

Then, we investigated the mechanism by which bFGF significantly boosted the formation of new blood vessels. Pioneering studies on the mechanism of therapeutic MSCs in diabetic wound healing provided some of the earliest findings that MSCs could directly differentiate into vascular endothelial cells and epidermal cells, promote the secretion of associated growth factors, and regulate cellular autophagy to prevent apoptosis.<sup>8,24</sup>

To elucidate whether transplanted MSCs could directly differentiate into vascular endothelial cells to promote the neovascularization, CM-Dil-labeled MSCs were transplanted into the wound site through subcutaneous injection or being loaded on a bioinspired collagen scaffold to cover the wound site. We found that injected MSCs remain in the superficial wound area while bioinspired collagen scaffold loaded MSCs infiltrated into deep skin tissue at wound sites. Co-staining with  $\alpha$ -SMA (marker of blood vessels) and S100A4 (marker of fibroblasts) showed that CM-Dil-labeled MSCs did not overlap the  $\alpha$ -SMA or S100A4 positive cells. Our evidence was not consistent with some previous literature and did not support that

the transplanted MSCs directly differentiated into vascular endothelial cells to promote the neovascularization in diabetic wound healing. Thus, we believed that the transplanted MSCs or bFGF-MSCs promoted the formation of new blood vessels through paracrine action.

Bioinformatics analysis of genomic transcriptional data between MSCs and bFGF-MSCs was performed to further explore the mechanism of boosting neovascularization by bFGF-MSCs. KEGG and GO analyses revealed that bFGF overexpression in MSCs led to a variety of gene and molecular changes distributed in signal pathways of cell proliferation and angiogenesis, suggesting that these might be the key pathways in accelerating diabetic wound healing following the treatment of bioinspired collagen scaffold loading bFGF-MSCs. Subsequent Western blotting assay confirmed that, for *in vitro* ECs, the supernatant released from bFGF-MSCs cultured on bioinspired collagen scaffold could increase phosphorylation of AKT and have a lasting increase in the expressions of HIF-1 $\alpha$  and HIF-1 $\beta$ . A previous study had showed that UC-MSCs upregulated platelet endothelial cell adhesion molecules and VEGF expression, promoting neovascularization through activating the phosphatidylinositol 3-kinase/Akt (PI3K-AKT) signaling pathway in wound healing.<sup>25</sup> The activation of AKT is a critical regulator of cell survival, proliferation, and migration, and is vital for wound healing.<sup>41,42</sup> Furthermore, phosphorylated AKT could influence the stability and activity of HIF1, enhancing the expression and activity of HIF-1 $\alpha$  and HIF-1 $\beta$ . HIF1, a key transcription factor under hypoxic conditions, is responsible for activating a variety of genes related to angiogenesis and cellular metabolism.<sup>43,44</sup> In the process of diabetic wound healing, promoting HIF1 activation could accelerate the formation of new blood vessels, improving blood circulation and oxygen supply in the wound area.<sup>45,46</sup> The wound healing process in diabetic patients is often delayed, partly due to insufficient angiogenesis, chronic inflammation, and abnormalities in the insulin signaling pathway.<sup>47</sup> The diabetic patient's hyperglycemic environment leads to increased degradation of HIF-1 $\alpha$ , inhibiting HIF-1 activity, which in turn impedes the wound healing process. By enhancing the HIF-1 signaling pathway, these negative effects can be reversed, promoting angiogenesis and tissue repair.<sup>48</sup> Basic fibroblast growth factor (bFGF) can enhance the HIF-1 signaling pathway by upregulating the expression and stability of HIF-1 $\alpha$ .<sup>49</sup> Our study found that the MSC scaffold loaded with bFGF significantly accelerated the healing of diabetic skin wounds. By measuring the expression levels of HIF-1 $\alpha$  and downstream genes, we demonstrated that the HIF-1 signaling pathway plays a crucial role in this process. The experimental results showed that the bFGF-MSC scaffold increased the stability of HIF-1 $\alpha$ , enhanced the expression of angiogenic factors, such as VEGF, and promoted the formation of new blood vessels and wound healing. The application of bFGF-MSCs in combination with the bioinspired skin collagen scaffold may help overcome these obstacles by activating the AKT-HIF1 signal pathway, promoting angiogenesis, and accelerating the wound healing process.

## CONCLUSION

In summary, our bioinspired collagen scaffold loaded with bFGF-MSCs markedly accelerated diabetic wound healing, mainly attributed to boosting angiogenesis via activating the AKT and -HIF1 signal pathway, providing strong evidence for combined applications of bioinspired skin regenerative materials

and engineered stem cells aiming for specific targets in further clinic use.

## ASSOCIATED CONTENT

### Data Availability Statement

All data generated or analyzed during this study are included in this published article. The data sets analyzed during the study are available from the corresponding author on reasonable request.

### Supporting Information

The Supporting Information is available free of charge at <https://pubs.acs.org/doi/10.1021/acsami.4c08174>.

The Supporting Information describes the construction of bFGF-MSCs and the use of ELISA to screening the MSCs capable of secreting the highest levels of bFGF. It also includes the quality evaluation of bFGF-MSCs through flow cytometry. Additionally, the information details the blood glucose levels of rats before and after STZ treatment (PDF)

## AUTHOR INFORMATION

### Corresponding Authors

**Yahong Huang** — School of Life Science, Nanjing University, Nanjing 210008 Jiangsu Province, China; Email: [hyh518@nju.edu.cn](mailto:hyh518@nju.edu.cn)

**Li Ling** — Department of Endocrinology, The Sixth Affiliated Hospital of Shenzhen University Medical School and Huazhong University of Science and Technology Union Shenzhen Hospital, Shenzhen 518020, China; Email: [lingli2018@email.szu.edu.cn](mailto:lingli2018@email.szu.edu.cn)

**Bin Wang** — Clinical Stem Cell Center, The Affiliated Drum Tower Hospital of Nanjing University Medical School, Nanjing 210008, China; Jiangsu Key Laboratory for Molecular Medicine, Nanjing University, Nanjing 210008 Jiangsu Province, China; [orcid.org/0000-0003-3981-8849](https://orcid.org/0000-0003-3981-8849); Email: [wangbin022800@126.com](mailto:wangbin022800@126.com)

### Authors

**Feifei Huang** — Clinical Stem Cell Center, The Affiliated Drum Tower Hospital of Nanjing University Medical School, Nanjing 210008, China

**Tianyun Gao** — Clinical Stem Cell Center, The Affiliated Drum Tower Hospital of Nanjing University Medical School, Nanjing 210008, China

**Yirui Feng** — School of Life Science, Nanjing University, Nanjing 210008 Jiangsu Province, China

**Yuanyuan Xie** — Clinical Stem Cell Center, The Affiliated Drum Tower Hospital of Nanjing University Medical School, Nanjing 210008, China

**Chenxu Tai** — Clinical Stem Cell Center, The Affiliated Drum Tower Hospital of Nanjing University Medical School, Nanjing 210008, China

Complete contact information is available at: <https://pubs.acs.org/10.1021/acsami.4c08174>

### Author Contributions

<sup>†</sup>F.H. and T.G. contributed equally to this work. B.W., F.H., and T.G. designed the study. F.H. and Y.F. carried out the isolation and culture of human HUCMSCs. F.H. and T.G. performed the other experiments and analyzed and formatted the data. F.H. wrote the first draft of the manuscript and all authors read, edited, and approved the final manuscript.



## Funding

This study was supported by National Natural Science Foundation of China (NSFC) [81571213 and 82070459 (Bin Wang)], Key Project of Jiangsu Province (Grant No. BE2020765) (Bin Wang), Project of Modern Hospital Management and Development Institute, Nanjing University/Aid project of Nanjing Drum Tower Hospital Health, Education & Research Foundation (NDYG2020030) (Bin Wang), Medical Research Foundation of Guangdong Province No:A2023181(Li Ling), Shenzhen Nanshan District Science and Technology Plan Foundation No: NS2023038 (Li Ling), and Research Foundation of Huazhong University of Science and Technology Union Shenzhen Hospital No: 2020024 (Li Ling).

## Notes

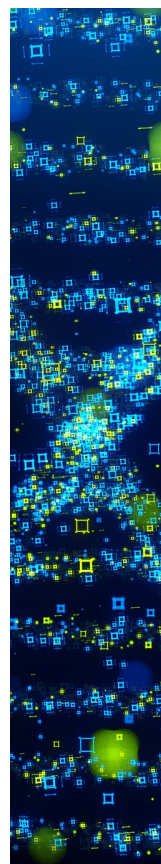
Ethics approval and consent to participate. All samples were procured after donors were well informed and signed written consent. The study was approved by the Research Ethics Board of Nanjing Drum Tower Hospital (permit number: 2017-161-01).

The authors declare no competing financial interest.

## REFERENCES

- (1) Patel, S.; Srivastava, S.; Singh, M. R.; Singh, D. Mechanistic insight into diabetic wounds: Pathogenesis, molecular targets and treatment strategies to pace wound healing. *Biomed Pharmacother* **2019**, *112*, No. 108615.
- (2) Xiao, J.; Zhu, Y.; Huddleston, S.; Li, P.; Xiao, B.; Farha, O. K.; Ameer, G. A. Copper Metal-Organic Framework Nanoparticles Stabilized with Folic Acid Improve Wound Healing in Diabetes. *ACS Nano* **2018**, *12* (2), 1023–1032.
- (3) Armstrong, D. G.; Boulton, A. J. M.; Bus, S. A. Diabetic Foot Ulcers and Their Recurrence. *N Engl J. Med.* **2017**, *376* (24), 2367–2375.
- (4) Boulton, A. J.; Vileikyte, L.; Ragnarson-Tennvall, G.; Apelqvist, J. The global burden of diabetic foot disease. *Lancet* **2005**, *366* (9498), 1719–24.
- (5) Singh, M. R.; Saraf, S.; Vyas, A.; Jain, V.; Singh, D. Innovative approaches in wound healing: trajectory and advances. *Artif Cells Nanomed Biotechnol* **2013**, *41* (3), 202–12.
- (6) Goldman, R. Growth factors and chronic wound healing: past, present, and future. *Adv. Skin Wound Care* **2004**, *17* (1), 24–35.
- (7) Yu, F. X.; Lee, P. S. Y.; Yang, L.; Gao, N.; Zhang, Y.; Ljubimov, A. V.; Yang, E.; Zhou, Q.; Xie, L. The impact of sensory neuropathy and inflammation on epithelial wound healing in diabetic corneas. *Prog. Retin Eye Res.* **2022**, *89*, 101039.
- (8) Han, Y.; Sun, T.; Tao, R.; Han, Y.; Liu, J. Clinical application prospect of umbilical cord-derived mesenchymal stem cells on clearance of advanced glycation end products through autophagy on diabetic wound. *Eur. J. Med. Res.* **2017**, *22* (1), 11.
- (9) Saadh, M. J.; Ramirez-Coronel, A. A.; Saini, R. S.; Arias-Gonzales, J. L.; Amin, A. H.; Gavilan, J. C. O.; Sarbu, I. Advances in mesenchymal stem/stromal cell-based therapy and their extracellular vesicles for skin wound healing. *Hum Cell* **2023**, *36* (4), 1253–1264.
- (10) McGee, G. S.; Davidson, J. M.; Buckley, A.; Sommer, A.; Woodward, S. C.; Aquino, A. M.; Barbour, R.; Demetriou, A. A. Recombinant basic fibroblast growth factor accelerates wound healing. *J. Surg Res.* **1988**, *45* (1), 145–53.
- (11) Choi, S. M.; Ryu, H. A.; Lee, K. M.; Kim, H. J.; Park, I. K.; Cho, W. J.; Shin, H. C.; Choi, W. J.; Lee, J. W. Development of Stabilized Growth Factor-Loaded Hyaluronate- Collagen Dressing (HCD) matrix for impaired wound healing. *Biomater Res.* **2016**, *20*, 9.
- (12) Choi, S. M.; Lee, K. M.; Kim, H. J.; Park, I. K.; Kang, H. J.; Shin, H. C.; Baek, D.; Choi, Y.; Park, K. H.; Lee, J. W. Effects of structurally stabilized EGF and bFGF on wound healing in type I and type II diabetic mice. *Acta Biomater* **2018**, *66*, 325–334.
- (13) Kuang, S.; He, F.; Liu, G.; Sun, X.; Dai, J.; Chi, A.; Tang, Y.; Li, Z.; Gao, Y.; Deng, C.; Lin, Z.; Xiao, H.; Zhang, M. CCR2-engineered mesenchymal stromal cells accelerate diabetic wound healing by restoring immunological homeostasis. *Biomaterials* **2021**, *275*, 120963.
- (14) Ren, Y.; Aierken, A.; Zhao, L.; Lin, Z.; Jiang, J.; Li, B.; Wang, J.; Hua, J.; Tu, Q. hUC-MSCs lyophilized powder loaded polysaccharide ulvan driven functional hydrogel for chronic diabetic wound healing. *Carbohydr. Polym.* **2022**, *288*, 119404.
- (15) Wu, Y.; Chen, L.; Scott, P. G.; Tredget, E. E. Mesenchymal stem cells enhance wound healing through differentiation and angiogenesis. *Stem Cells* **2007**, *25* (10), 2648–59.
- (16) O'Loughlin, A.; Kulkarni, M.; Creane, M.; Vaughan, E. E.; Mooney, E.; Shaw, G.; Murphy, M.; Dockery, P.; Pandit, A.; O'Brien, T. Topical administration of allogeneic mesenchymal stromal cells seeded in a collagen scaffold augments wound healing and increases angiogenesis in the diabetic rabbit ulcer. *Diabetes* **2013**, *62* (7), 2588–94.
- (17) Liu, W.; Xie, Y.; Gao, T.; Huang, F.; Wang, L.; Ding, L.; Wang, W.; Liu, S.; Dai, J.; Wang, B. Reflection and observation: cell-based screening failing to detect HBV in HUMSCs derived from HBV-infected mothers underscores the importance of more stringent donor eligibility to reduce risk of transmission of infectious diseases for stem cell-based medical products. *Stem Cell Res. Ther* **2018**, *9* (1), 177.
- (18) Huang, F.; Gao, T.; Wang, W.; Wang, L.; Xie, Y.; Tai, C.; Liu, S.; Cui, Y.; Wang, B. Engineered basic fibroblast growth factor-over-expressing human umbilical cord-derived mesenchymal stem cells improve the proliferation and neuronal differentiation of endogenous neural stem cells and functional recovery of spinal cord injury by activating the PI3K-Akt-GSK-3 $\beta$  signaling pathway. *Stem Cell Res. Ther* **2021**, *12* (1), 468.
- (19) Tai, C.; Xie, Z.; Li, Y.; Feng, Y.; Xie, Y.; Yang, H.; Wang, L.; Wang, B. Human skin dermis-derived fibroblasts are a kind of functional mesenchymal stromal cells: judgements from surface markers, biological characteristics, to therapeutic efficacy. *Cell Biosci* **2022**, *12* (1), 105.
- (20) Lim, J. Z.; Ng, N. S.; Thomas, C. Prevention and treatment of diabetic foot ulcers. *J. R Soc. Med.* **2017**, *110* (3), 104–109.
- (21) Guillamat-Prats, R. The Role of MSC in Wound Healing, Scarring and Regeneration. *Cells* **2021**, *10* (7), 1729.
- (22) Fang, S.; Xu, C.; Zhang, Y.; Xue, C.; Yang, C.; Bi, H.; Qian, X.; Wu, M.; Ji, K.; Zhao, Y.; Wang, Y.; Liu, H.; Xing, X. Umbilical Cord-Derived Mesenchymal Stem Cell-Derived Exosomal MicroRNAs Suppress Myofibroblast Differentiation by Inhibiting the Transforming Growth Factor- $\beta$ /SMAD2 Pathway During Wound Healing. *Stem Cells Transl Med.* **2016**, *5* (10), 1425–1439.
- (23) Sharma, P.; Kumar, A.; Dey, A. D.; Behl, T.; Chadha, S. Stem cells and growth factors-based delivery approaches for chronic wound repair and regeneration: A promise to heal from within. *Life Sci.* **2021**, *268*, 118932.
- (24) Han, Y. F.; Sun, T. J.; Han, Y. Q.; Xu, G.; Liu, J.; Tao, R. Clinical perspectives on mesenchymal stem cells promoting wound healing in diabetes mellitus patients by inducing autophagy. *Eur. Rev. Med. Pharmacol Sci.* **2015**, *19* (14), 2666–70.
- (25) Zhang, S.; Chen, L.; Zhang, G.; Zhang, B. Umbilical cord-matrix stem cells induce the functional restoration of vascular endothelial cells and enhance skin wound healing in diabetic mice via the polarized macrophages. *Stem Cell Res. Ther* **2020**, *11* (1), 39.
- (26) Wang, Z.; Qi, F.; Luo, H.; Xu, G.; Wang, D. Inflammatory Microenvironment of Skin Wounds. *Front Immunol* **2022**, *13*, 789274.
- (27) Gadelkarim, M.; Abushouk, A. I.; Ghanem, E.; Hamaad, A. M.; Saad, A. M.; Abdel-Daim, M. M. Adipose-derived stem cells: Effectiveness and advances in delivery in diabetic wound healing. *Biomed Pharmacother* **2018**, *107*, 625–633.
- (28) Richard, J. L.; Parer-Richard, C.; Dures, J. P.; Clouet, S.; Vannereau, D.; Bringer, J.; Rodier, M.; Jacob, C.; Comte-Bardonnet, M. Effect of topical basic fibroblast growth factor on the healing of chronic diabetic neuropathic ulcer of the foot. A pilot, randomized, double-blind, placebo-controlled study. *Diabetes Care* **1995**, *18* (1), 64–9.

- (29) Uchi, H.; Igarashi, A.; Urabe, K.; Koga, T.; Nakayama, J.; Kawamori, R.; Tamaki, K.; Hirakata, H.; Ohura, T.; Furue, M. Clinical efficacy of basic fibroblast growth factor (bFGF) for diabetic ulcer. *Eur. J. Dermatol* **2009**, *19* (5), 461–8.
- (30) Serna, N.; Cano-Garrido, O.; Sanchez, J. M.; Sanchez-Chardi, A.; Sanchez-Garcia, L.; Lopez-Laguna, H.; Fernandez, E.; Vazquez, E.; Villaverde, A. Release of functional fibroblast growth factor-2 from artificial inclusion bodies. *J. Controlled Release* **2020**, *327*, 61–69.
- (31) Hao, W.; Han, J.; Chu, Y.; Huang, L.; Zhuang, Y.; Sun, J.; Li, X.; Zhao, Y.; Chen, Y.; Dai, J. Collagen/Heparin Bi-Affinity Multilayer Modified Collagen Scaffolds for Controlled bFGF Release to Improve Angiogenesis In Vivo. *Macromol. Biosci* **2018**, *18* (11), No. e1800086.
- (32) Zubair, M.; Ahmad, J. Role of growth factors and cytokines in diabetic foot ulcer healing: A detailed review. *Rev. Endocr Metab Disord* **2019**, *20* (2), 207–217.
- (33) Singer, A. J.; Clark, R. A. Cutaneous wound healing. *N Engl J. Med.* **1999**, *341* (10), 738–46.
- (34) King, A. J. The use of animal models in diabetes research. *Br. J. Pharmacol.* **2012**, *166* (3), 877–94.
- (35) Sun, Y.; Weber, K. T. Infarct scar: a dynamic tissue. *Cardiovasc. Res.* **2000**, *46* (2), 250–6.
- (36) Gurtner, G. C.; Werner, S.; Barrandon, Y.; Longaker, M. T. Wound repair and regeneration. *Nature* **2008**, *453* (7193), 314–21.
- (37) Mi, B.; Chen, L.; Xiong, Y.; Yan, C.; Xue, H.; Panayi, A. C.; Liu, J.; Hu, L.; Hu, Y.; Cao, F.; Sun, Y.; Zhou, W.; Liu, G. Saliva exosomes-derived UBE2O mRNA promotes angiogenesis in cutaneous wounds by targeting SMAD6. *J. Nanobiotechnology* **2020**, *18* (1), 68.
- (38) Li, Y.; Wang, J.; Qian, D.; Chen, L.; Mo, X.; Wang, L.; Wang, Y.; Cui, W. Electrospun fibrous sponge via short fiber for mimicking 3D ECM. *J. Nanobiotechnology* **2021**, *19* (1), 131.
- (39) Chang, M.; Nguyen, T. T. Strategy for Treatment of Infected Diabetic Foot Ulcers. *Acc. Chem. Res.* **2021**, *54* (5), 1080–1093.
- (40) Daub, J. T.; Merks, R. M. A cell-based model of extracellular-matrix-guided endothelial cell migration during angiogenesis. *Bull. Math Biol.* **2013**, *75* (8), 1377–99.
- (41) Manning, B. D.; Cantley, L. C. AKT/PKB signaling: navigating downstream. *Cell* **2007**, *129* (7), 1261–74.
- (42) Song, G.; Ouyang, G.; Bao, S. The activation of Akt/PKB signaling pathway and cell survival. *J. Cell Mol. Med.* **2005**, *9* (1), 59–71.
- (43) Zhang, Z.; Yao, L.; Yang, J.; Wang, Z.; Du, G. PI3K/Akt and HIF-1 signaling pathway in hypoxia-ischemia (Review). *Mol. Med. Rep* **2018**, *18* (4), 3547–3554.
- (44) Lee, S. H.; Golinska, M.; Griffiths, J. R. HIF-1-Independent Mechanisms Regulating Metabolic Adaptation in Hypoxic Cancer Cells. *Cells* **2021**, *10* (9), 2371.
- (45) Li, G.; Ko, C. N.; Li, D.; Yang, C.; Wang, W.; Yang, G. J.; Di Primo, C.; Wong, V. K. W.; Xiang, Y.; Lin, L.; Ma, D. L.; Leung, C. H. A small molecule HIF-1 $\alpha$  stabilizer that accelerates diabetic wound healing. *Nat. Commun.* **2021**, *12* (1), 3363.
- (46) Zhu, Y.; Wang, Y.; Jia, Y.; Xu, J.; Chai, Y. Roxadustat promotes angiogenesis through HIF-1 $\alpha$ /VEGF/VEGFR2 signaling and accelerates cutaneous wound healing in diabetic rats. *Wound Repair Regen* **2019**, *27* (4), 324–334.
- (47) Dasari, N.; Jiang, A.; Skochdopole, A.; Chung, J.; Reece, E. M.; Vorstenbosch, J.; Winocour, S. Updates in Diabetic Wound Healing, Inflammation, and Scarring. *Semin Plast Surg* **2021**, *35* (3), 153–158.
- (48) Guo, J.; Hu, Z.; Yan, F.; Lei, S.; Li, T.; Li, X.; Xu, C.; Sun, B.; Pan, C.; Chen, L. Angelica dahurica promoted angiogenesis and accelerated wound healing in db/db mice via the HIF-1 $\alpha$ /PDGF- $\beta$  signaling pathway. *Free Radic Biol. Med.* **2020**, *160*, 447–457.
- (49) Rao, Z.; Shen, D.; Chen, J.; Jin, L.; Wu, X.; Chen, M.; Li, L.; Chu, M.; Lin, J. Basic Fibroblast Growth Factor Attenuates Injury in Myocardial Infarction by Enhancing Hypoxia-Inducible Factor-1 Alpha Accumulation. *Front Pharmacol* **2020**, *11*, 1193.



CAS BIOFINDER DISCOVERY PLATFORM™

## STOP DIGGING THROUGH DATA —START MAKING DISCOVERIES

CAS BioFinder helps you find the  
right biological insights in seconds

Start your search

**CAS**  
A division of the  
American Chemical Society